Kinetics of aggregation in non-Brownian magnetic particle dispersions in the presence of perturbations

F. Donado[1]
Instituto de Ciencias Básicas e Ingeniería-CIMA, Universidad Autónoma del Estado de Hidalgo, Pachuca 42090, Pachuca, México

U. Sandoval and J. L. Carrillo
Instituto de Física de la Universidad Autónoma de Puebla, Apartado Postal J-48, Puebla 72570, Puebla, México
(Received 29 October 2008; published 26 January 2009)

An experimental and theoretical study on the kinetics of the aggregation process of magnetic particles dispersed in mineral oils is presented. A static magnetic field and an oscillating magnetic perturbation are applied on the dispersion. In the low-particle concentrations, the effects on the aggregation of the frequency, the concentration of particles and the viscosity of the liquid are analyzed. It was found that the behavior of the cluster length as a function of the main control parameters can be accurately characterized by scaling relations. The physical characteristics of the aggregates are discussed in relation to measurements of viscosity as a function of time.

DOI: 10.1103/PhysRevE.79.011406 PACS number(s): 61.43.Hv, 45.50.−j, 83.80.Gv

I. INTRODUCTION

Complex liquids composed by micrometric magnetic particles dispersed in inert oils, usually called magnetorheological (MR) fluids, and in the presence of a magnetic field exhibit macroscopic transformations and physical properties that can be modulated by means of the intensity of the applied field [1–7]. Clearly this is due to the formation of clusters by the dispersed particles. In the low-particle concentration regime, the clusters are chainlike in shape and oriented in the direction of the applied field [1–3]. The length of these clusters is determined by particle size and concentration, liquid viscosity, and intensity of the applied field. For dilute dispersions of brownian particles in the absence of fluxes, the clusters are built mainly by two aggregation mechanisms: axial aggregation and lateral aggregation. These mechanisms act at different time scales. The first mechanism acts immediately when a magnetic field is applied, in a time scale of milliseconds. The magnetic field induces a dipolar moment in the particles, causing the particles to interact and attract each other to form elongated chain-shaped clusters. The second mechanism consists of thermally activated chain aggregation. It is a slower mechanism. Thermal fluctuations in the liquid produce small deformations in the chains and a derived movement. Due to the lateral component of the local field, the chains interact and aggregate to generate longer and thicker chains [3,8–11].

When the dispersion is subject to a small shear stress, its rheological behavior can be closely associated and described in terms of the dynamics of the aggregation process, in the sense the effective viscosity of dispersion strongly depends on the length and thickness of the chains. In this way, the rheological behavior suffers strong changes at short times when the magnetic field is applied due to the axial aggregation of particles, and slower changes due to lateral aggregation of chains. Under certain physical conditions, the changes induced at long time scales by lateral aggregation can be as important as those induced at short time scales by axial aggregation.

Nevertheless, to our knowledge, only two studies have addressed the discussion on how external agents can hasten and enhance the lateral aggregation of chains formed by particles in order to modify the rheological behavior of a MR fluid [7,12]. In Ref. [7], Tao describes a procedure to hasten the lateral aggregation of chains, based on the application of a sudden pressure increment in the MR fluid. By this means, Tao observed the formation of thicker clusters and higher yield stress values. In Ref. [12], we have recently proposed a procedure to hasten the lateral aggregation of chains in a magnetorheological dispersion of non-Brownian particles. Basically, this procedure consists of exposing the rheological dispersion simultaneously to a static magnetic field and a low amplitude oscillating magnetic field as a perturbation. The perturbation field induces a waving movement in the chains formed by the fields. These chain movements favor lateral interactions, which induce the aggregation of chains to form larger chains or chains with thicker structures, depending on their relative position, in a way remarkably more intense and faster than that produced only by thermal fluctuations.

This work presents a comprehensive discussion of the effects of perturbation on the kinetics of the aggregation process, in terms of the average length of aggregates, under several conditions of perturbation frequency, liquid viscosity, and particle concentration. It also discusses the effect of perturbation on the viscosity behavior of a magnetorheological dispersion as a function of time. In Sec. II, we briefly describe the experimental procedures and setups, along with the experimental results. In Sec. III, we present a theoretical disscussion of the frequency dependence of the kinetics of the aggregation process in terms of the Mason number. Finally in Sec. IV, some remarks and comments are made.

II. EXPERIMENTAL

The experimental study was performed on samples of different particle concentrations prepared with magnetite par-

*Corresponding author. fernando@uaeh.edu.mx

ticles having an average size of 65 μm and a standard dispersion of 15 μm; the magnetite powder has a measured density of 5.1 g/cm^3. The powder was dispersed in a Dextron-type oil of viscosity 76 cP. The different stages of the aggregation process were observed by means of a Meiji EMZ-TR microscope. The aggregation process was recorded using a Diagnostic Instruments digital camera and a Sony HandyCam videocamera. The dispersion sample was poured into a rectangular glass cell 14 mm in width, 19 mm in length and in sufficient quantity to form a wet layer. The static and perturbation horizontal fields were generated by means of two couples of Helmholtz coils. One of the couples, with coil radius of 90 mm, generated the static field, the other, with coil radius of 70 mm, generated the oscillatory perturbation field. These fields were allocated in such a way so that they were perpendicular to each other. In this configuration, the mutual impedance effect was negligible. The couples were connected to a power supply controlled by a PC with a NI Instruments I/O card. In most of the measurements the r.m.s. amplitude of the perturbation field was kept to 15% of the static one. Due to the size and position of the sample with relation to the couples of Helmholtz coils, the applied effective field was essentially homogeneous. The viscosity measurements were made by means of a Brookfield DVLV III rheometer in the cone-plate geometry. The cone and plate that bounds the sample is made from a nonmagnetizable material. The static and perturbation fields were generated by the same couples of Helmholtz coils described above, allocated in such a way that the static field was vertical and the perturbation field was horizontal. In order to keep the sample at 20 °C, a Brookfield thermal bath was used.

A. Particle magnetization measurements

When only a static field is acting on a magnetorheological dispersion subject to a shear rate perpendicular to the applied field, there exist a critical value of the shear rate which distinguishes between a regime dominated by the magnetic force and another regime dominated by the viscous force. This value of the shear rate also is related to a structural transformation similar to a phase transition in which the dispersion goes from an isotropic phase to a nematiclike one [13]. The physical conditions in which this transformation occurs can be established quantitatively in terms of a coefficient known as the Mason number Ma. This is defined as the ratio between magnetic force and dissipative force due to the liquid viscosity. When the Mason number is larger than the unit, the nematic-like phase is observed, and if it is less than the unit, the isotropic phase is present. Thus, the critical condition is described by Ma=1. In a rheogram $\dot{\gamma}-\tau$, this structural isotropic-nematic transition is observed as an abrupt change in the slope at a critical shear rate [13].

It was possible to use the critical shear rate $\dot{\gamma}_c$ to estimate the magnitude of magnetization of particles used in our experiments. To this end, we basically followed the derivation of the Mason number as proposed in Ref. [14]. Nevertheless, we replaced in the Stokes force the term $v=\omega a$, for a pair of particles in a MR fluid under a rotating magnetic field [14], by $v=\dot{\gamma}a$, for a pair of particles in a MR fluid under a static field and shearing [13]. It yielded a Mason number given by

$$\mathrm{Ma}=\frac{12^2\eta\dot{\gamma}}{\mu_0 M^2}, \tag{1}$$

where M is particle magnetization, η is liquid viscosity, and $\dot{\gamma}$ is shear rate. From this equation, given Ma=1, one obtains for particle magnetization

$$M=\sqrt{\frac{12^2\eta\dot{\gamma}_c}{\mu_0}}. \tag{2}$$

We have carried out rheological measurements around the isotropic-nematic transition in a MR fluid sample at several magnetic field intensities using a Bohlin CVO rheometer in the cone-plate geometry. The magnetic field was provided by a solenoid placed around the sample. Figure 1(a) shows the behavior of the critical shear rate as a function of H, the magnetic field intensity. A power law behavior can adequately describe the experimental data, $\dot{\gamma}_c \sim H^\beta$, being $\beta \approx 1$ in our experiments. Using Eq. (2) and the explicit power law for $\dot{\gamma}_c$, a magnetization curve for the material particles can be found, as shown in Fig. 1(b).

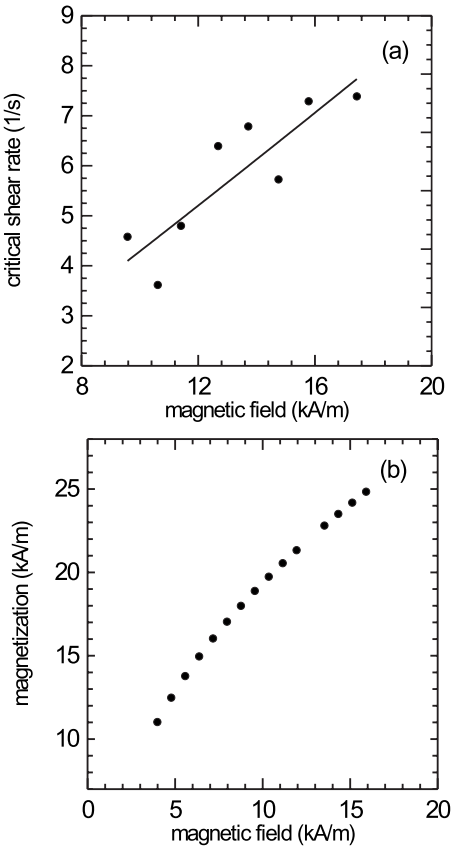

FIG. 1. (a) Critical shear rate as a function of the magnetic field, the continuous line is the fitting by a power law. (b) Magnetization curve obtained by using the experimental power law for the critical shear rate and the relation of magnetization given by Eq. (2).

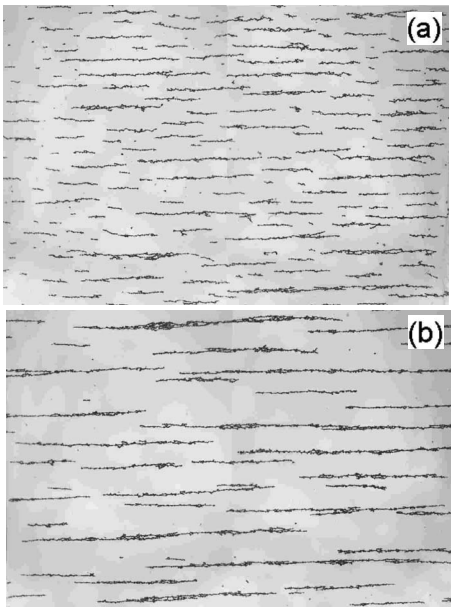

FIG. 2. (a) Chain-shaped clusters when a 92 G static field is applied on the sample. (b) Chains when in addition to a 80 G static field is applied a transversal 12 G r.m.s perturbation. Both photographs were taken 200 s after the fields were turned on.

B. Magnetic perturbation effects

Figure 2 shows a comparison of two kinds of chain-shaped clusters. One formed as a result of the application of a static field of 92 G, Fig. 2(a), and the other formed as a result of the application of a static field of 80 G as well as a magnetic perturbation of amplitude 12 G r.m.s. and 2 Hz frequency, Fig. 2(b). The average length was clearly larger when both fields were present. Thus, the perturbation field had an impressively strong effect on the length of the resulting clusters. Certainly this should be important in the rheological properties of dispersion.

The time behavior of the average cluster length was taken in this work as the central quantity in order to discuss the kinetics of the aggregation process under several physical conditions. To analyze the time behavior of the cluster length in the sample, the experimental procedure used was as follows. Once a sample of MR dispersion was prepared, it was left to stand for 5 min for the particles to sediment. In this quasi-two-dimensional system, the particles occupied a surface area of 0.05. Video sequences were taken under various different conditions, starting some time before the fields were applied and throughout 200 s in the presence of fields. From these videos, some photographs were taken at certain time intervals to measure the length of the clusters. In all samples, the layer of clusters are formed in a plane.

Figure 3 shows typical log-log curves of the average length of the aggregates as a function of time in the presence of both fields. The curve (a) corresponds to a sample under a 80 G static field and a 12 G r.m.s. transversal perturbation with 1.5 Hz frequency. For curve (b), the sample is under a 80 G static field and a transversal 12 G, 12 Hz perturbation field. Finally, for curve (c), the sample is under a 80 G static field, plus 12 G transversal static field. It is clear from the

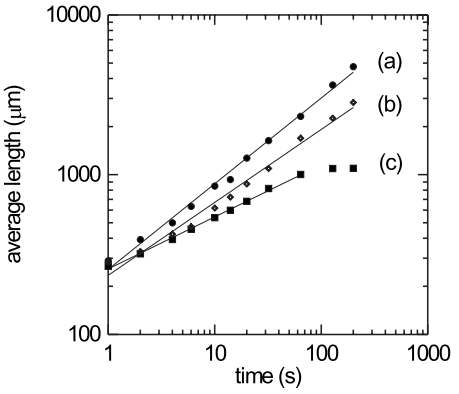

FIG. 3. Average length as a function of time for several conditions: (a) 80 G static field and a 12 G r.m.s. transversal perturbation with 1.5 Hz frequency. (b) 80 G static field and a transversal 12 G, 12 Hz perturbation field. (c) 80 G static field, plus 12 G transversal static field. Each continuous line is the fitting by a power law.

figure that the time behavior of the average length of the chains, when the transversal field oscillates, is a scaling relation given by a well-defined power law $\bar{L} \sim t^{\alpha}$. For the conditions of Fig. 3 in curves (a) and (b), the exponents are $\alpha = 0.53$ and $\alpha = 0.45$, respectively. The curve (c) shows a scaling relation below the time $t = 64$ s; its exponent is 0.32.

It was observed that, for the given liquid viscosity, particle concentration, intensity of the static field, and amplitude of perturbation, the variability of perturbation expressed in its frequency f_p has an important effect on the aggregation. It is reasonable to expect that for the given conditions there must exist a frequency of perturbation that would optimize the aggregation, leading to larger and thicker chains. A graph of the average length of clusters as a function of the frequency of perturbation is shown in Fig. 4. The general feature of this dependence is that, initially, the average length increases with frequency, reaching its maximum for a frequency around 2 Hz, then it shows a clear decreasing behavior. The physical meaning of crossover frequency and its relationship with dissipation shall be discussed below. The

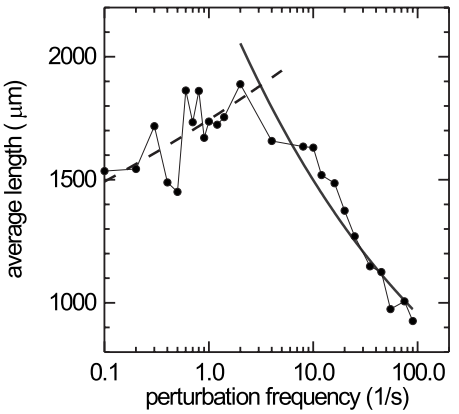

FIG. 4. Average length of the chain-shaped clusters as a function of the frequency of perturbation. There is a critical behavior around the frequency of 2 Hz: to the left the data is fitted by an increasing power law; to the right the data is fitted by a decreasing power law.

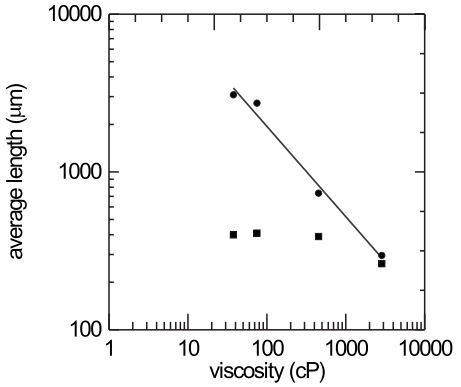

FIG. 5. Comparison of the average length of aggregates for various viscosities of the liquid for a sample exposed to a static field and a perturbation (circles), and when the sample is exposed only to a static field (squares). The continuous line is the fitting by a power law.

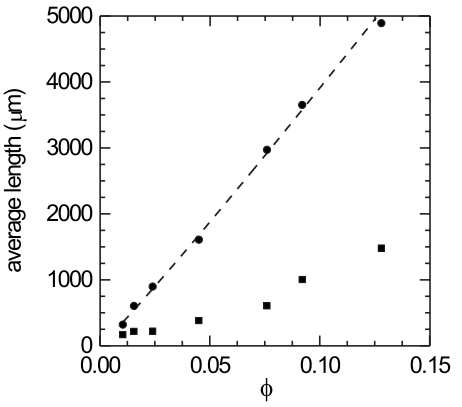

FIG. 6. Comparison of the length of aggregates for various particle concentrations: a sample exposed to a static field and a perturbation field (circles) and the same sample exposed only to a static field (squares). The dashed line is the fitting by a power law.

dashed line is the fitting by a power law $\bar{L} \sim f_p^{\delta_i}$ for the increasing part, $\delta_i = 0.066$. The thicker continuous line is the fitting by a power law $\bar{L} \sim f_p^{\delta_d}$ for the decreasing portion $\delta_d = -0.1962$. The two power laws intercept around 3 Hz. The thin continuous line is to guide the eye.

The liquid viscosity also determines to some extent the average length of clusters. Obviously, there exists a complex interrelation with other physical quantities in the system, such as particle concentration and amplitude and frequency of perturbation. Figure 5 shows the comparison of the average length of clusters as a function of liquid viscosity, after 200 s the fields have been in action. For this series of experiments, we used Cannon standard silicon oils. The upper set of dots, which admits fitting by a power law $\bar{L} \sim \eta^{\psi}$, shows the behavior of the average length when the sample is acted by a 80 G static field and a 12 G r.m.s., 2 Hz, magnetic perturbation, $\psi = -0.5722$, for our experimental conditions. The set of squares represents the behavior of the average length when there is only a 80 G static field acting on the system. As expected the efficiency of perturbation to enhance the lateral aggregation of chains decreases with the viscosity of the liquid.

One should expect that the process of lateral aggregation of chains, caused by perturbation, must be affected by particle concentration. This is so because the fast aggregation of particles caused by the fields should generate a large number of chains for larger values of particle concentration. Figure 6 shows that when the sample is exposed to perturbation, there is a power law that fits the average length with particle concentration $\bar{L} \sim \phi^{\xi}$ for our experimental conditions $\xi = 1.059$. For the case in which the sample is only exposed to a static field, the increase in average length with particle concentration is slower. For larger values of particle concentration, this dependence departs from the scaling behavior. It can be associated with the fact that the cluster structure at that condition becomes more complex [5]; this is so for both cases, namely in the presence and in the absence of perturbation.

Rheological measurements were performed under not exactly but close to the same conditions of sample geometry and applied field geometry as the images of chain aggregation. The main differences were the confinement imposed by the cone and plate geometry, and the small but not zero shearing over the sample. We have observed that perturbation frequency and particle concentration have important effects on the effective viscosity of dispersion. Figure 7 shows the measured effective viscosity of a sample with a particle concentration of 0.05 in volume fraction and a cone angular speed of 1 RPM. The comparison is among three perturbation frequencies, 2 Hz (dots), 1 Hz (squares), and 0.5 Hz (circles). Each experiment consisted of four stages. Initially, the sample is subjected to a shear rate in the absence of fields; then, during the first 200 s the sample acts only under a 80 G static field; after that, a 12 G r.m.s. perturbation is applied along 300 s; and finally, during the last 240 s perturbation is suppressed. Note that in the time interval in which both fields were acting, the sample where the frequency of perturbation was 2 Hz underwent larger increments in its effective viscosity.

Figure 8 shows the effects of particle concentration on effective viscosity. In the three curves, initially during a time interval of 180 s, only the 2 Hz perturbation frequency with

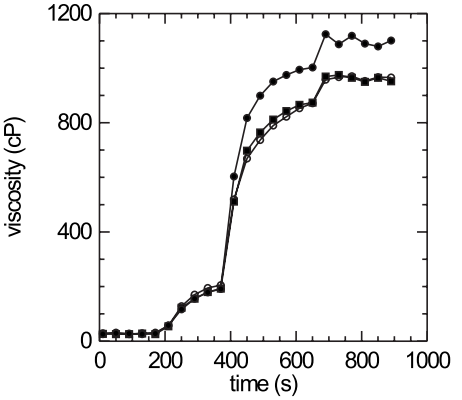

FIG. 7. Comparison of the measured effective viscosities as a function of time for three values of perturbation frequency: 2 Hz (dots), 1 Hz (squares), and 0.5 Hz (circles). Continuous lines are for eye guiding purposes. For details see text.

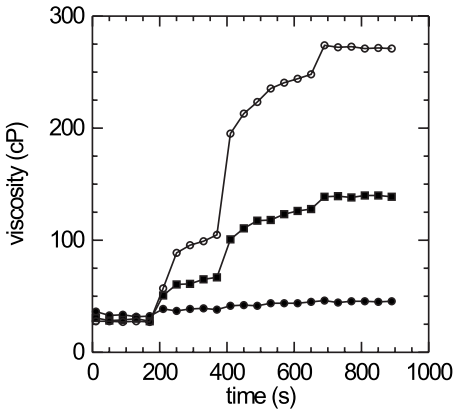

FIG. 8. Time behavior of effective viscosity for three volume particle concentrations: 0.005 (dots), 0.02 (squares), and 0.03 (circles). Continuous lines are guides for the eye.

a cone angular speed of 2 RPM is acting. Then, during 200 s the 80 G static field is turned on. In this interval, differences are caused by particle concentration: 0.005 (dots), 0.02 (squares), and 0.03 (circles). During the following 300 s, in addition to the shear rate and the static field, a 12 G r.m.s. is applied on the system. Note that during this interval the rheological response of the sample with the lowest concentration is practically negligible. Finally, during the following 240 s, the perturbation field is suppressed. As expected, the larger the particle concentration, the larger the rheological change caused by the applied fields.

In the last segment of the curves from Figs. 7 and 8, an interesting effect is observed that, when perturbation is suppressed viscosity increases. This unexpected effect reflects that for these concentrations, the viscosity of the liquid combined with perturbation acts as a limitation at the end of the process of chain growth. Likewise, the viscous force counteracting the movements of the chains caused by waving and shearing break the chains at some critical length. This is why when perturbation is suppressed these portions of chains aggregate again, increasing the length and thickness of the chains and consequently the effective viscosity of dispersion.

III. THEORETICAL DISCUSSION

A. A differential form for the average length of the aggregates

From the above sections, it is clear that the dependence of the average length of the aggregates on several of the external relevant parameters admits a description based on scaling relations. Taking advantage of this, it is possible to write a differential form to describe the increment of the average cluster length as a function of the relevant variables, namely, the time t, the surface fraction occupied by the particles ϕ, the frequency of perturbation f_p, and the liquid viscosity η. Considering these dependencies $\bar{L}=\bar{L}(t,\phi,f_p,\eta)$ and the scaling relations discussed above, most of the characteristics of the behavior of the average length of clusters as a function of control parameters can be established by means of the following differential form:

$$dL = \sum (A_i \epsilon_i X_i^{\epsilon_i - 1}) dX_i, \tag{3}$$

where ϵ_i stands for the exponent of the power law corresponding to the scaling of L with the variable X_i; the latter labels the variables which the average length depends on.

Of course it is necessary to specify the range in which the scaling relation holds valid for the different variables. For the system studied here the ranges are established as in Table I.

TABLE I. Ranges in which the scaling relations hold valid for the different variables.

Variable	Valid range
ϕ	0.01–0.09
η	37–2860 cP
f_p	0–90 Hz
t	0–200 s

B. Magnetization and dissipation

As discussed above, the distribution of particles may be considered as a 2D distribution inside the wetting layer. Under these conditions, the particles are exposed to an effective magnetic field given by

$$\vec{H}_{\text{ef}} = [H_c \hat{i} + H_p \sin(2\pi f_p t)\hat{j}], \tag{4}$$

where H_c is the intensity of the static field, here arbitrarily taken in the x direction. H_p is the amplitude of the oscillatory field conceived as a perturbation, and f_p is its frequency. Due to the applied field, the particles acquire a magnetic moment $\vec{m}$ oriented in the direction of the effective field $\vec{H}_{\text{ef}}$. Consider spherical particles $\vec{m}=\frac{3\pi a^3}{4}\vec{M}$, where $\vec{M}$ is magnetization and a is particle diameter. The particle magnetization in terms of the magnetic field is given by $\vec{M}=\chi_p \vec{H}_{\text{ef}}$, with χ_p as the effective magnetic susceptibility of the particles. In this way, the particle magnetization can be written in the form

$$\vec{M} = \chi_p [H_c \hat{i} + H_p \sin(2\pi f_p t)\hat{j}]. \tag{5}$$

On the other hand, the potential energy between two dipolar particles is given by the expression

$$U = -\frac{\mu_0}{4\pi}\left(\frac{3(\vec{r}\cdot\vec{m})^2}{r^5} - \frac{m^2}{r^3}\right), \tag{6}$$

where $\vec{r}$ is the separation between particles. Then, the magnetic force between two particles is given by

$$\vec{F}^m = \frac{3\mu_0}{4\pi}\left[\left(\frac{m^2}{r^5} - \frac{5(\vec{r}\cdot\vec{m})^2}{r^7}\right)\vec{r} + \frac{2(\vec{r}\cdot\vec{m})}{r^5}\vec{m}\right]. \tag{7}$$

Since the particles move through the liquid, we also consider the Stokes viscous force given by

$$\vec{F}^{\text{vis}} = 6\pi\eta a \vec{V}, \tag{8}$$

η being the liquid viscosity and $\vec{V}$ the particle speed in the fluid.

By using these quantities as well as the magnetization discussed above, Sec. II A, it is now possible to analyze the role of the dissipation of energy provided by perturbation due to liquid viscosity. Thermal effects are negligible as can

be seen by the comparison of the average energy associated to the liquid thermal fluctuations with magnetic energy. Let λ be this rate for the magnetic interaction of the two particles and thermal energy. If it would happen that $\lambda \gg 1$, then the thermal fluctuations may be neglected. From Eq. (6), one can see that the magnetic energy for two joint particles, along the static field direction, is given by $W_m = \frac{\mu_0 \pi a^3 M^2}{9}$, where $r=2a$. Thus, λ is given by

$$\lambda = \frac{W_m}{kT} = \frac{\pi \mu_0 a^3 M^2}{9 k_B T}, \tag{9}$$

where k_B is the Boltzmann's constant and T is thermodynamic temperature. Since the average size of the particles used in this study is 65 μm and from the values of magnetization given in Sec. II A, one finds that $\lambda \approx 10^9$. Therefore, the thermal fluctuations are negligible.

As shown by Fig. 4, the combined effect of perturbation and liquid viscosity imposes a limitation in the average length of the clusters. Now the physical explanation of this phenomenon shall be discussed by comparing viscous and magnetic interactions. The perturbation field produces a waving movement of chains, transversal to the direction of the static field. Obviously, this movement takes place against the viscous force. To evaluate the effect of this on the kinetics of aggregation and average length and thickness of those chains, it could be useful to adapt the definition of the Mason number given in Ref. [14]. In that paper, to study the behavior of dispersion of non-Brownian magnetic particles with magnetization M in a liquid with viscosity η exposed to a rotating magnetic field of frequency w, the Mason number can be cast into

$$\mathrm{Ma} = \frac{12^2 \eta w}{\mu_0 M^2}. \tag{10}$$

To arrive at this expression, one shall consider the ratio between viscous force and magnetic force between two joint particles. The viscous force is obtained from Eq. (8) by using $v=wa$. The magnetic force is given by Eq. (7) taking $r=2a$. For dispersions in the presence of a rotating field, it has been found that there is a crossover Mason number Ma=1, above which the rotation of fields prevents particle aggregation from forming chains [2].

In our experiments, we have observed that under the action of perturbation, the chains show a waving movement in which their extremes oscillate around the static field direction. Here it is assumed that the chains can be modeled as straight arrangements of particles whose extremes follow the resultant field $\vec{H}_{\mathrm{ef}} = [H_c \hat{i} + H_p \sin(2\pi f_p t)\hat{j}]$. The angle of oscillation with respect to the direction of the static field as a function of time is given by $\psi = \psi_{\max} \sin(2\pi f_p t)$; then the angular speed is

$$\omega = 2\pi f_p \psi_{\max} \cos(2\pi f_p t). \tag{11}$$

The maximum of this quantity $\omega_{\max}$ is given by

$$\omega_{\max} = 2\pi f_p \psi_{\max}. \tag{12}$$

The average angular speed in a semiperiod is the average of Eq. (11) in this time interval, given by

TABLE II. Critical perturbation frequency for different magnetic fields using $\omega_{\max}$ and $\bar{\omega}$, see text.

H_c (kA/m)	f_{p_c} (1/s) [using $\omega_{\max}$]	f_{p_c} (1/s) [using $\bar{\omega}$]
3.978	1.097377794	1.723761039
4.774	1.407862663	2.211470671
5.570	1.715347395	2.694467688
6.366	2.020419893	3.173675568
7.161	2.323477253	3.649718069
7.957	2.624805606	4.123044647
8.753	2.924620852	4.593994434
9.549	3.223091621	5.062832319
10.345	3.520353225	5.529770846
11.140	3.816516607	5.994984286
11.936	4.111674356	6.458618078
13.528	4.699275497	7.38162195
14.323	4.991844471	7.841189295
15.119	5.283662858	8.299577618
15.915	5.574775691	8.756857656

$$\bar{\omega} = 4 f_p \psi_{\max}. \tag{13}$$

The angle $\psi_{\max}$ can be determined by the expression $\psi_{\max} = \tan^{-1}(H_p/H_c)$, H_p being the amplitude of the perturbation field. For the values $H_c = 80$ G and $H_p = 17$ G used in this study, $\psi_{\max} = 0.209264$ rad.

Now we use the values of $\bar{\omega}$ and $\omega_{\max}$ to determine each one a Mason number for the system and look for which one of them better describes the oscillatory chain kinetics. The explict Mason number obtained using $\omega_{\max}$ is

$$\mathrm{Ma} = \frac{288 \eta \pi f_p \psi_{\max}}{\mu_0 M^2}. \tag{14}$$

Experimentally we have found that there exists a crossover or critical perturbation frequency $f_{p_c} \approx 2$ Hz. Above that, the average chain length decreases with the frequency following a power law relationship, and below it the average chain length increases with frequency following a different power law. We expected that this f_{p_c} is closely related to the physical conditions in which the Mason number equals the unit.

From Eq. (14) one obtains an expression for f_{p_c}, provided that Ma=1, as

$$f_{p_c} = \frac{\mu_0 M^2}{12^2 \eta 2 \pi \psi_{\max}}. \tag{15}$$

If one uses the results for magnetization discussed in the above section, one arrives at the values of crossover frequency for different intensities of applied static fields. These are presented in Table II.

For the calculation of f_{p_c}, we have only considered the amplitude of the static field because the maximun angular speed is reached when the magnetic perturbation intensity vanishes instantaneously. For the conditions of the experiments discussed here, one can estimate that the crossover

frequency is 2.02 Hz. Notice that, fortunately, this value is very close to the experimental value $f_p=2$ Hz for which the average length reaches the maximun value, as seen in Fig. 4. Furthermore, if one uses the average value of angular speed $\bar{\omega}$ to obtain the crossover frequency, one obtains 3.1 Hz. This is approximately the value of frequency at the point of intersection of the lines of the power laws fitted to the average length as a function of frequency, as it was discussed with relation to Fig. 4.

Notice that the power delivered to the chains by magnetic perturbation dissipates via viscous effects into the liquid. Thus, the Raleigh dissipation function can be used to estimate this rate of transfer of energy into the liquid

$$\Upsilon = \int \vec{F}^{\text{vis}} \cdot d\vec{V} \approx 3\pi\eta a \bar{V}^2, \tag{16}$$

where the average value of the speed of particles in the chain has been approximated by $\bar{V}=\bar{\omega}a=a4f_p\psi_{\max}$, as obtained from Eq. (13).

IV. COMMENTS AND REMARKS

The main facts of our experiments are the following. In the low-particle concentration regime, the cluster formed as a result of particle aggregation under perturbations are chain shaped. When the static and perturbation fields are applied, the chains are oriented in the effective magnetic field direction; therefore these oscillate in the transversal direction of the static field with perturbation frequency. The oscillation described here as a waving motion induced by perturbation becomes an extra mechanism in the kinetics of aggregation. This mechanism is as important as the mechanism of particle aggregation induced by direct dipolar interactions. In addition, the mechanism driven by magnetic perturbations seems to be effective both at the short time scales and at the long time scales. This fast aggregation process leads to rapid increments in the effective viscosity of dispersion. Finally, the induced aggregation by perturbation may be seen also as a mechanism to control viscosity at the long time scales. Given the liquid viscosity, intensity of the static field and amplitude of perturbation, there is a crossover value of the perturbation frequency which clearly separates the two regimes of lateral aggregation of chains. The average length of the aggregates depends on several variables; most of these dependencies show a scaling behavior.

ACKNOWLEDGMENTS

The partial financial support by PROMEP-SEP México under Grant No. 103.5/06/1275, CONACyT, México Grant No. 44296, and VIEP-UAP Grant No. 41/EXC/07-08 is acknowledged. Also U.S. was supported by CONACyT Grant No. CVU-211081.

[1] P. Domínguez-García, S. Melle, J. M. Pastor, and M. A. Rubio, Phys. Rev. E **76**, 051403 (2007).
[2] S. Melle, O. G. Calderon, M. A. Rubio, and G. G. Fuller, Phys. Rev. E **68**, 041503 (2003).
[3] E. M. Furst and A. P. Gast, Phys. Rev. E **62**, 6916 (2000).
[4] J. Vicente, M. T. López-López, J. D. G. Duran, and F. Gonzalez-Caballero, Rheol. Acta **44**, 94 (2004).
[5] J. L. Carrillo, F. Donado, and M. E. Mendoza, Phys. Rev. E **68**, 061509 (2003).
[6] S. Genc and P. Phulé, Smart Mater. Struct. **11**, 140 (2002).
[7] R. Tao, J. Phys.: Condens. Matter **13**, R979 (2001).
[8] J. E. Martin, Phys. Rev. E **63**, 011406 (2000).
[9] E. M. Furst and A. P. Gast, Phys. Rev. E **61**, 6732 (2000).
[10] S. Cutillas and J. Liu, Phys. Rev. E **64**, 011506 (2001).
[11] D. Wirtz and M. Fermigier, Phys. Rev. Lett. **72**, 2294 (1994).
[12] F. Donado, J. L. Carrillo, and M. E. Mendoza, J. Magn. Magn. Mater. **320**, e354 (2008).
[13] O. Volkova, S. Cutillas, and G. Bossis, Phys. Rev. Lett. **82**, 233 (1999).
[14] S. Melle, O. G. Calderón, G. G. Fuller, and M. A. Rubio, J. Colloid Interface Sci. **247**, 200 (2002).